



Daniele Gatti
Tutor: Prof. Pasquale Arpaia
XXXII Cycle – III year presentation

Low-cost transducer networks for real-time movement tracking



My Background

- Master degree in Electronic Engineering (cum laude) from University of Naples, “Federico II” (2016).
- PhD Student XXXII Cycle Information Technology and Electrical Engineering, DIETI (2017).
- Augmented Reality for Health Monitoring Laboratory.
- Type of Fellowship: No Grant



Credits Summary

➤ Credits Table

Student: Daniele Gatti		Tutor: Pasquale Arpaia		Cycle XXXII																						
daniele.gatti@unina.it		pasquale.arpaia@unina.it																								
	Credits year 1								Credits year 2								Credits year 3								Total	Check
	Estimated	1	2	3	4	5	6	Summary	Estimated	1	2	3	4	5	6	Summary	Estimated	1	2	3	4	5	6	Summary		
Modules	18			9	3		9	21	15							0	15				9			9	30	30-70
Seminars	13	1	7				0.6	8.6	5							0	5				3			3	11.6	10-30
Research	34	4.50	4.50	5.40	6.50	5.50	4.00	30.4	40	9.0	7.5	7.5	7.0	6.0	8.0	45.0	20	11.50	10.0	10.0	8.5	11.5	11.5	63.00	138.40	80-140
	65	5.50	11.50	14.40	9.50	5.50	13.60	60.00	60	9	7.5	7.5	7	6	8	45.0	40	11.5	10	10	21	12	12	75.00	180.00	180

All the established objects has been reached. Half of the second year was spent abroad (CERN Switzerland).



Content

- Indoor tracking

- State of the art
 - ❑ Technologies
 - ❑ Technique
 - ❑ Proposal: Hybrid heading and tracking system

- Realization
 - ❑ Filters and sensor board
 - ❑ Low-cost electronics goniometer

- Results

- Remarks

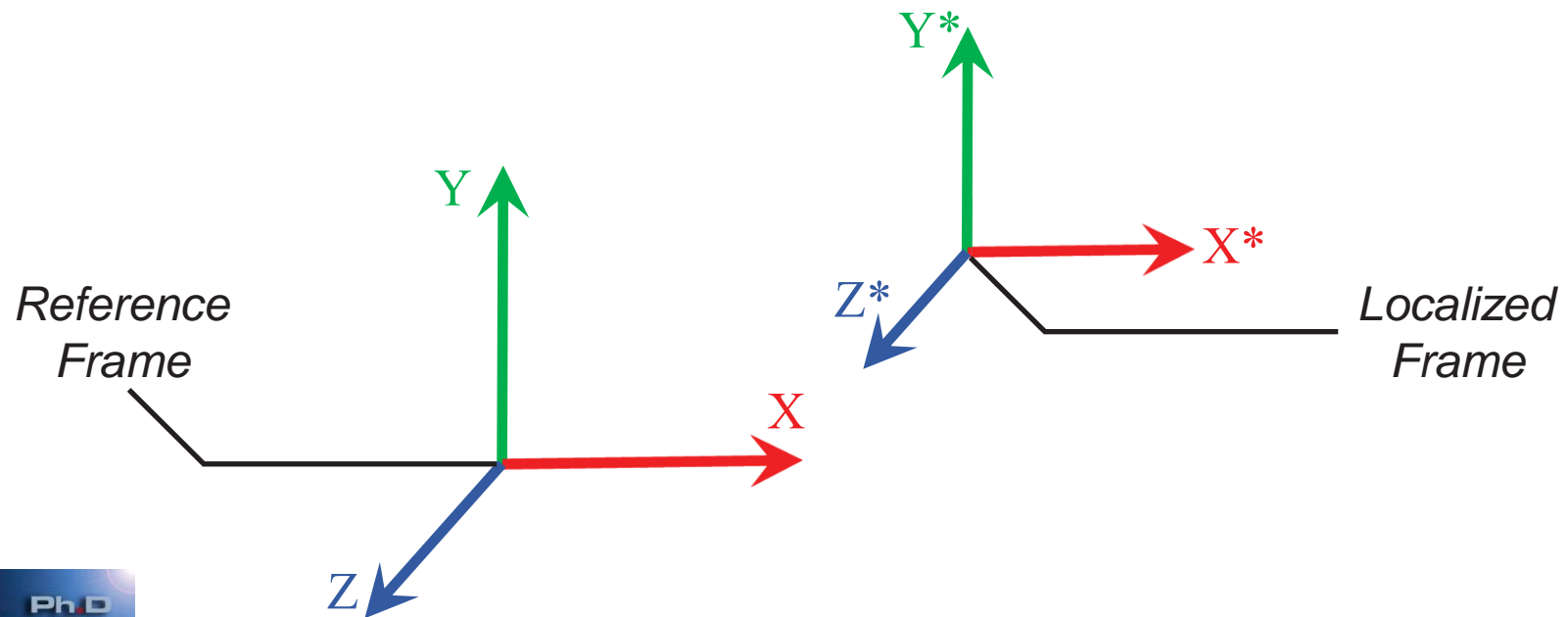
Indoor tracking



Indoor tracking

An indoor tracking system, measuring the position and orientation of a target with respect to a reference frame, in indoor environments.

The research concerns the use of **low-cost** transducers and microcontrollers for tracking.



Application

Many application needs to know the dynamic target position such as: domotics, augmented reality, robotics, assisted navigation in buildings, health systems, and objects localization. The outdoor localization technology are not applicable to the indoor environments due to the low accuracy (1-2 m) [1].

Virtual museum



Inspection robot

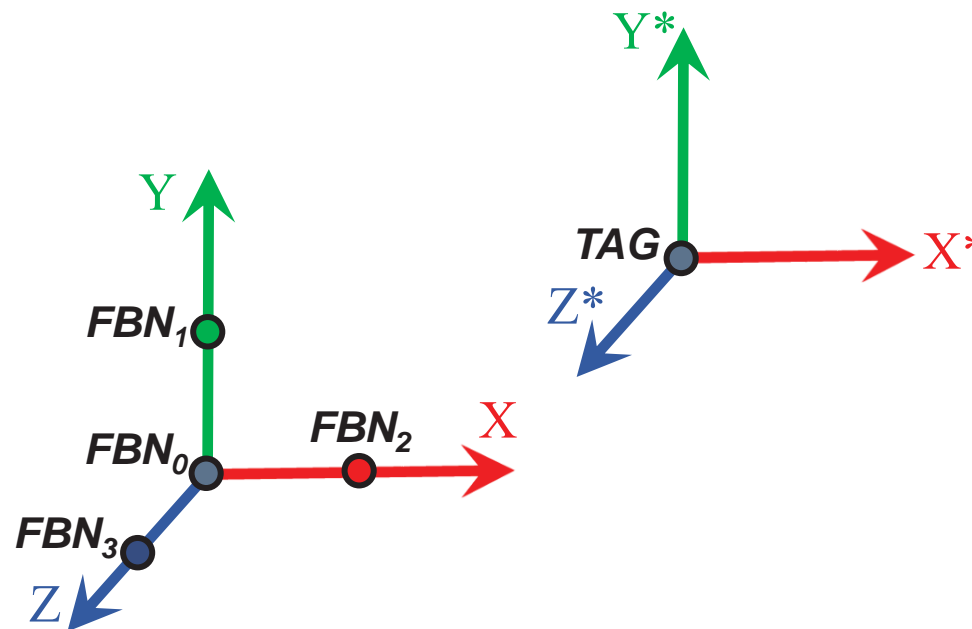


State of the art



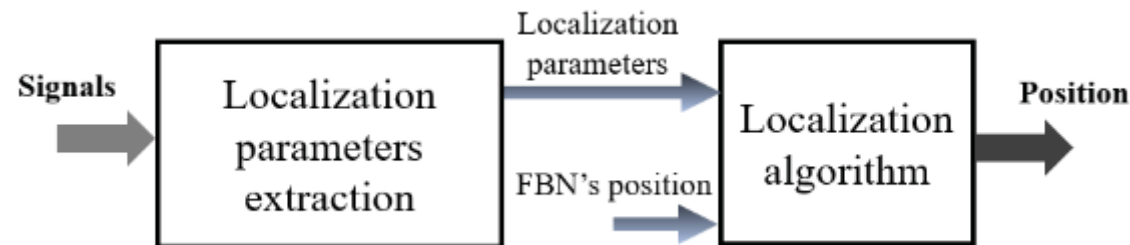
Position tracking

The reference frame contains N fixed beacon nodes (FBN_i) in known positions. The localized frame contains the unknown target node (TAG). By exploiting different localization techniques and technologies the TAG position can be estimated.



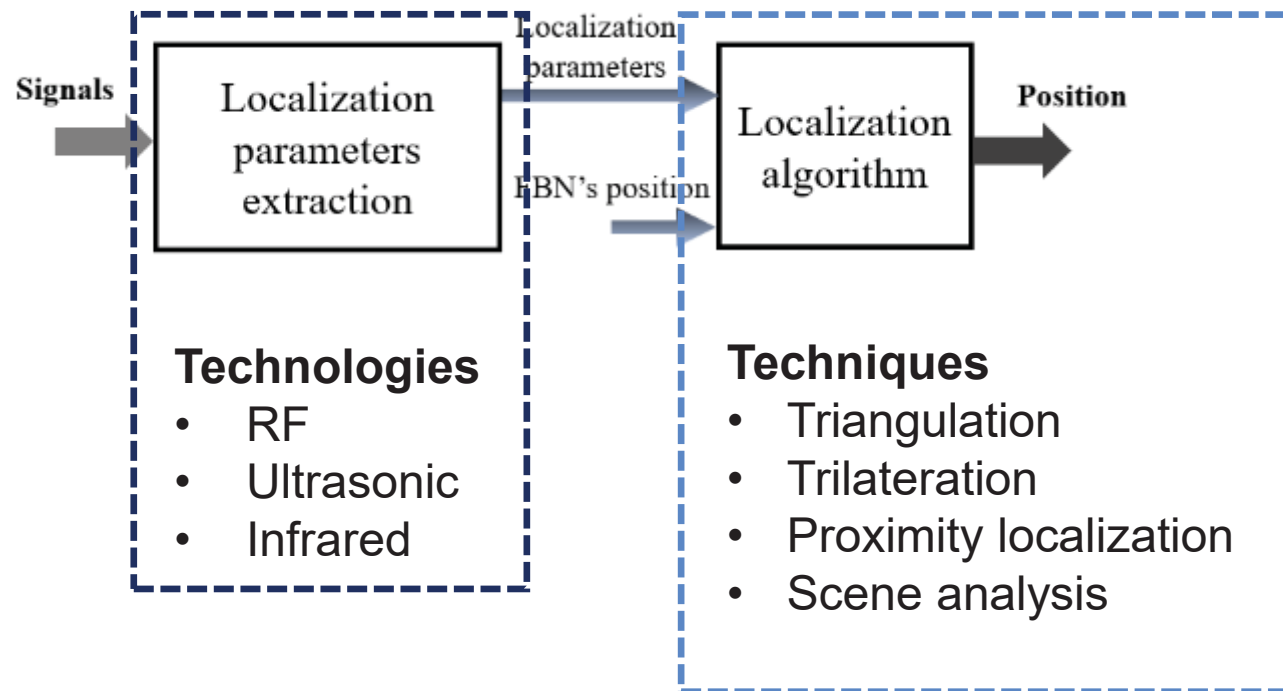
Position tracking

Position estimation can be divided into two different phases: the *localization parameters extraction* and *localization algorithm* calculation [2].



Position tracking

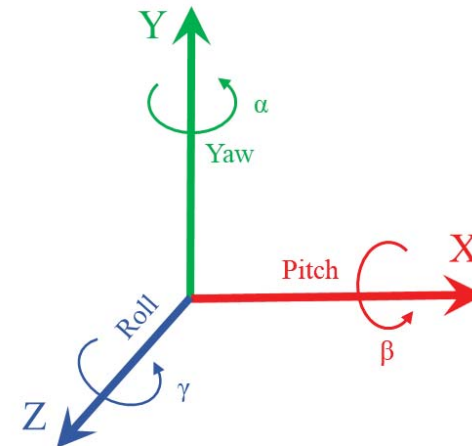
Position estimation can be divided into two different phases: the *localization parameters extraction* and *localization algorithm* calculation [2].



Inertial navigation

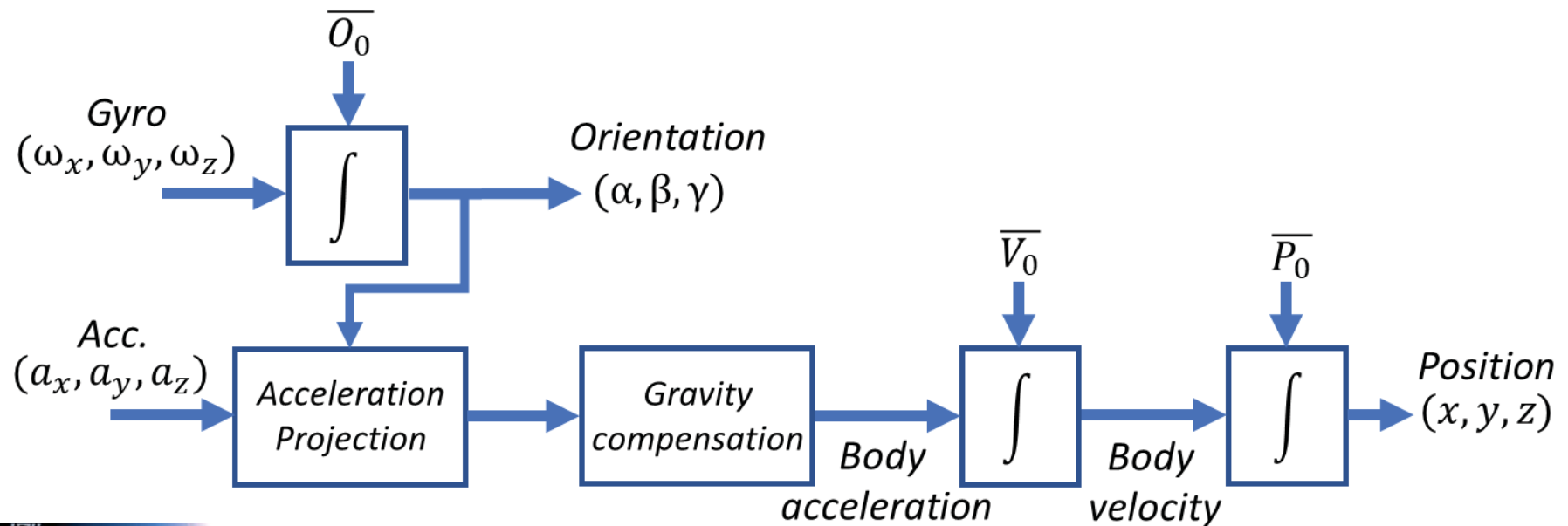
Inertial navigation, is a technique in which measurements provided by accelerometer and gyroscope are used to track the position and orientation.

The MEMS technology easily combine 3 axis gyroscope, accelerometer, and magnetometer all in the same package (9DOF). These chips, referred to as Inertial Measurements Unit (IMU).



Inertial navigation

The **gyroscope** measure the rotation rate of a body, while the **accelerometer** is a device which measures the velocity change rate of an acceleration with respect to the inertial frame of the object. The data acquired from those sensors have to be integrate over the time, in order to measure the position and orientation.



Inertial navigation

The presence of a bias and others errors in the sensors measurements, causing **drifting** in the position and orientation estimation during the integration. **Sensor Fusion** is needed [3].

- Common approach is to periodically correct drift using position data from an absolute positioning system (e.g. RF, Ultrasonic).
- The accelerometers were used to compensate the gyroscope drift for the **pitch** and **roll** measurements. For the **yaw** compensation the **magnetometer** sensor is needed.

$$\text{Calibration model: } \omega_{gyro} = a + b \omega_{true} \quad \text{Ideal Gyro: } a = 0, b = 1$$

$$\text{Angle error: } \epsilon(t) = \alpha_{gyro}(t) - \alpha_{true}(t) = \int_0^t \omega_{gyro} dt - \int_0^t \omega_{true} dt$$

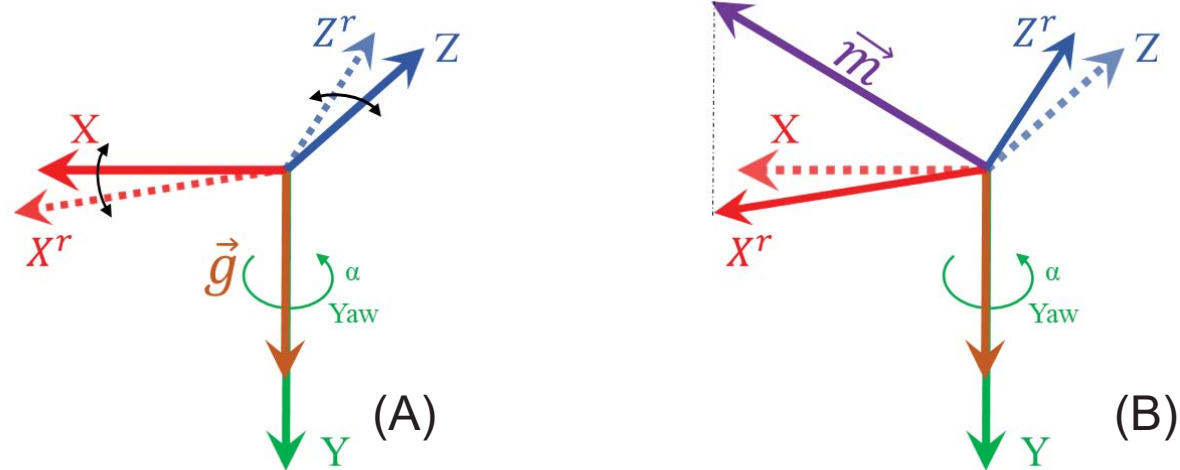
$$\omega_{true} = 0; \forall t \geq 0$$

$$\epsilon(t) = at$$

Drift error

Inertial navigation

The acceleration vector approximately points in the down direction of the **Earth frame**. Infinitely solutions exist for the yaw orientation (A).



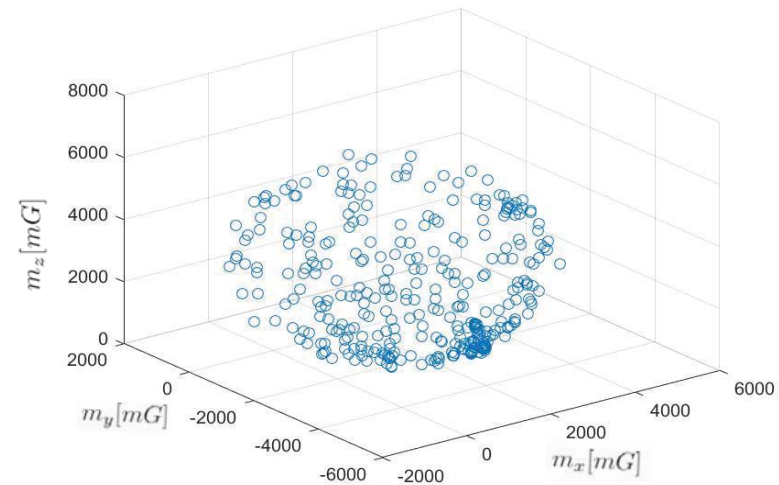
The earth magnetic field vector \vec{m} , points in a fixed direction in the **Earth frame** (the magnetic North), providing a single heading solution (B).

Inertial navigation

Materials that serve as a source of magnetic fields causing **hard iron disturbance**. Other materials distort the magnetic fields that pass through them causing **soft iron disturbance**.

Magnetometer calibration methods mainly take into account, *offsets* due to hard-iron bias and *eccentricities* due to soft-iron bias.

Raw data ST LIS3MDL
Magnetometer sensor



Inertial navigation

Offline calibration mitigates the magnetic disturbance for the most applicative cases. If the local magnetic configuration change, online calibration is needed [4]. In presence of strong magnetic field, the readings become dependent on small location changes. The magnetometer cannot produce useful outputs for the yaw drift error detection.

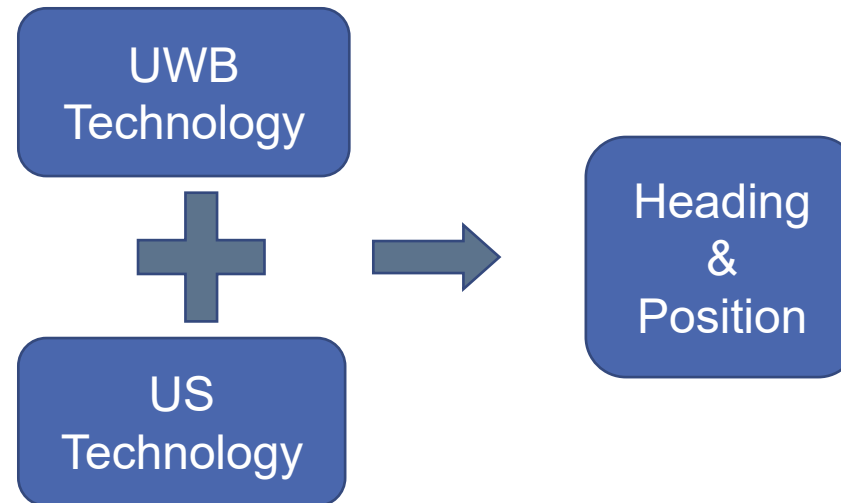


The CERNbot system during a test in front of a collimator of the LHC tunnel [5].

Proposed method

A magnetometer-less system, based on the combination of the ultrasonic (US) and ultra-wideband (UWB) technology, is proposed.

- Two US receiver sensor were used for the heading (yaw) estimation.
- The UWB system measure the distance, therefore the position can be estimated.

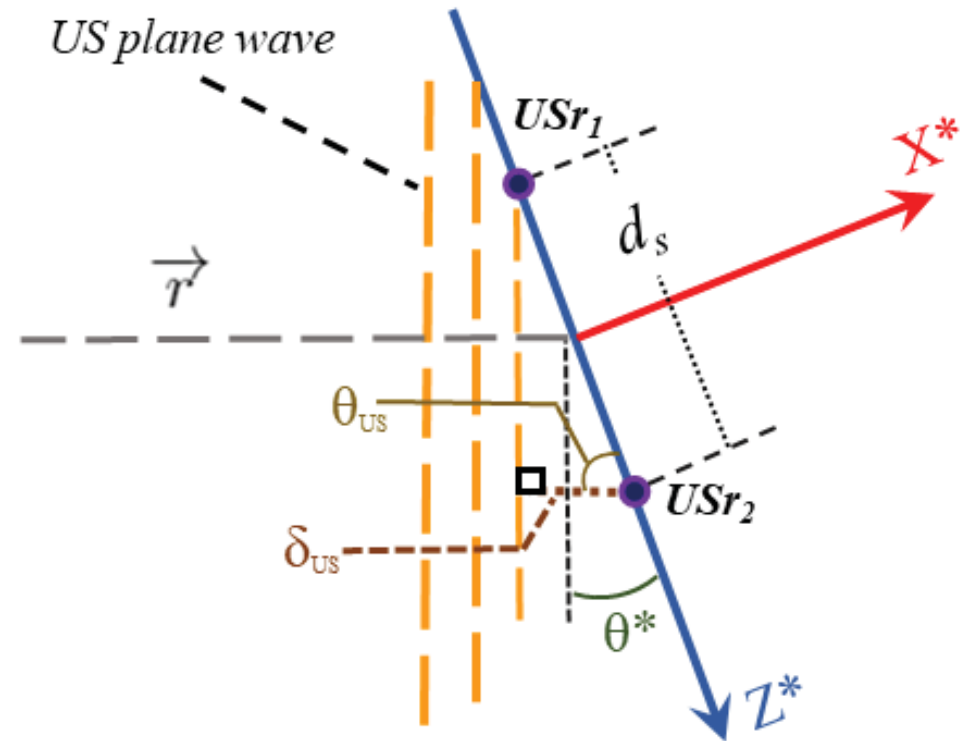


Measurements principle

θ^* heading angle estimation.

Condition:

- 2D Case study.
- Far field condition.
- Two element US linear array.



$$\theta^* = \frac{\pi}{2} - \underbrace{\arccos\left(\frac{\delta_{US}}{d_s}\right)}_{\theta_{US}} \rightarrow \begin{array}{l} \text{Measured distance} \\ \text{Known sensors distance} \end{array}$$

Measurements principle

Why UWB?

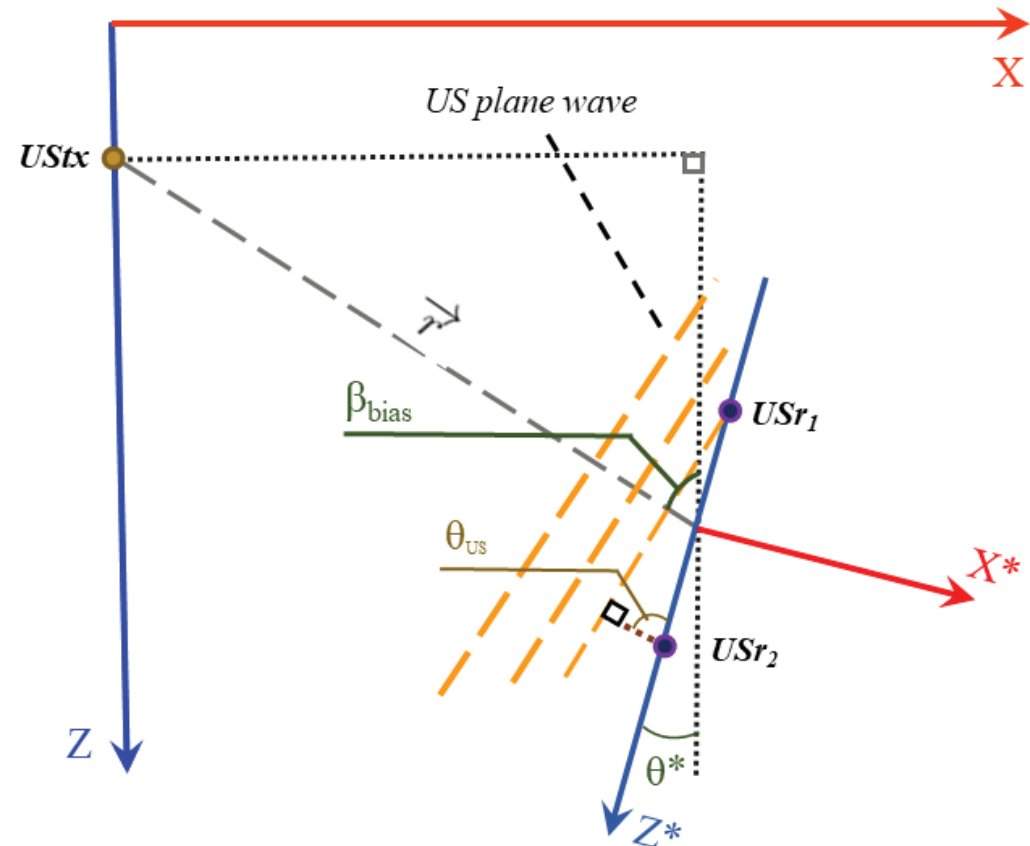
The displacement between the US emitter ($UStx$) causing a shift for the θ^* estimation.

$$\theta^* = \beta_{bias} - \arccos\left(\frac{\delta_{US}}{d_s}\right)$$

$$\beta_{bias} = \arccos\left(\frac{Z_* - Z_{tx}}{|\vec{r}|}\right)$$

Origin localized
frame position

$UStx$ Z
position



Measurements principle

Assuming a received sinusoidal plane wave, the output signal from the ultrasonic sensors are:

$$v_{chi}(t) = A_i \cos(2\pi f_s t + \varphi_i), i = 1, 2$$

The unknown distance is related to the zero crossing time difference

$$t_1 = \frac{\frac{\pi}{2} - \varphi_1}{2\pi} T; t_2 = \frac{\frac{\pi}{2} - \varphi_2}{2\pi} T \rightarrow \delta t = \frac{\varphi_2 - \varphi_1}{2\pi} T \quad \delta_{US} = v \delta t$$

The ambiguity phase is solved if: $\delta_{US} < \frac{\lambda}{2}$ Mechanical constraints

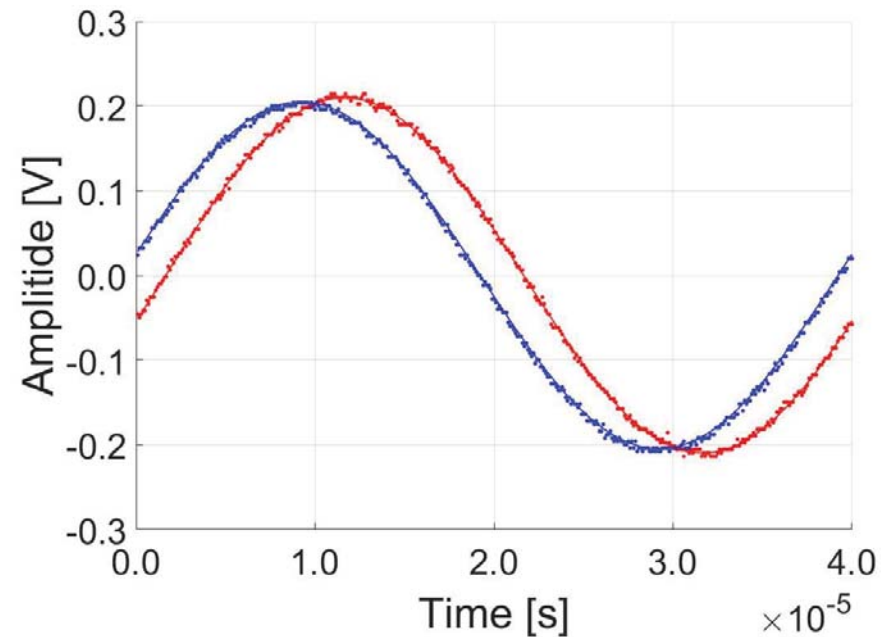
Measurements principle

The most simple technique for the phase shift measurements is the zero crossing.

- Limited accuracy (sample time).
- High noise sensibility [6].



Sine fit algorithm



Measurements principle

The standard three parameter sine-fit computing the best fit of a single tone sampled sinusoidal signal. The sine-fit inputs are the signal frequency and the sample rate. Low harmonic distortion is required [7].



Resonant transducer

The resonance frequency set the minimum receiver distance: $\delta_{US} < \frac{\lambda}{2}$
Considering a: $f_r = 25 \text{ kHz} \rightarrow \delta_{US} < 6.63 \text{ mm}$

- ✓ Commercial MEMS receivers dimension is: 2-3 [mm]

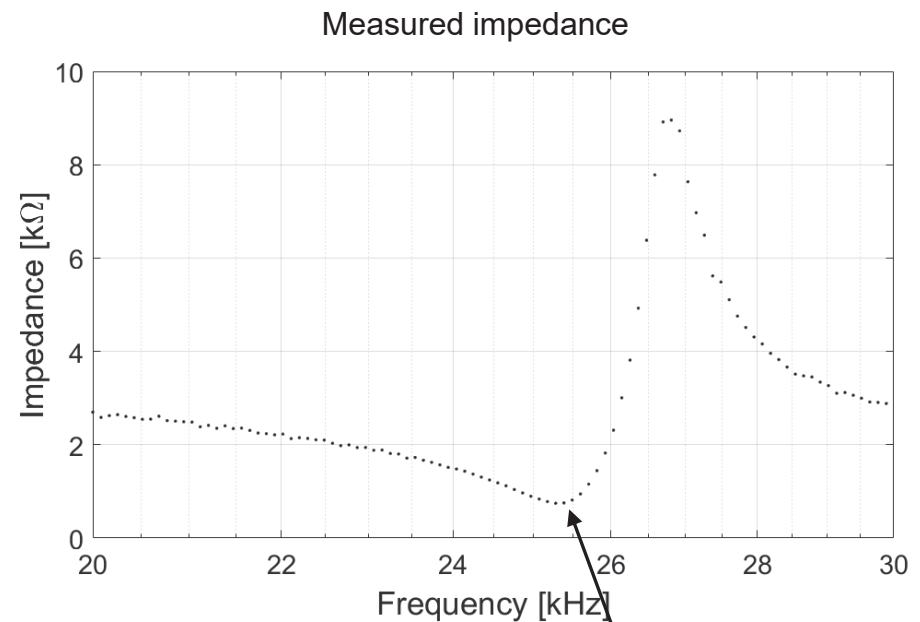
Realization



Realization

Transmitter: Prowave 250ST180.

- Low-cost piezoelectric transducer.
- Emitter aperture $D = 13.5 \text{ mm}$.
- Nominal resonance frequency $f_r = 25 \text{ kHz}$.
- Maximum applicable voltage $V_{max} = 15 V_{rms}$.

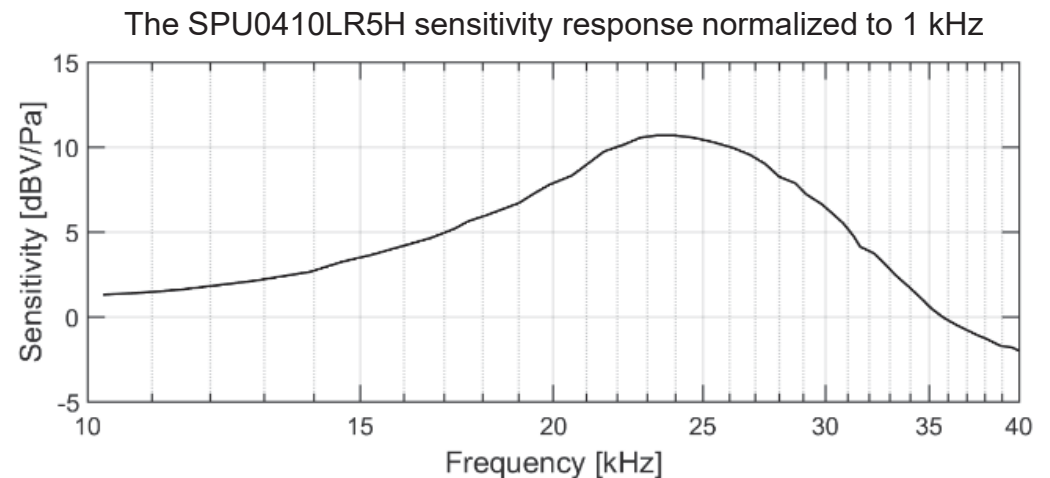
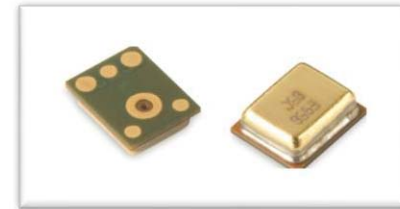


$$|Z(f = 24.5 \text{ kHz})| = 750 \Omega$$

Realization

Reicevers: MEMS SPU0410LR5H transducer. (Knowles Tech).

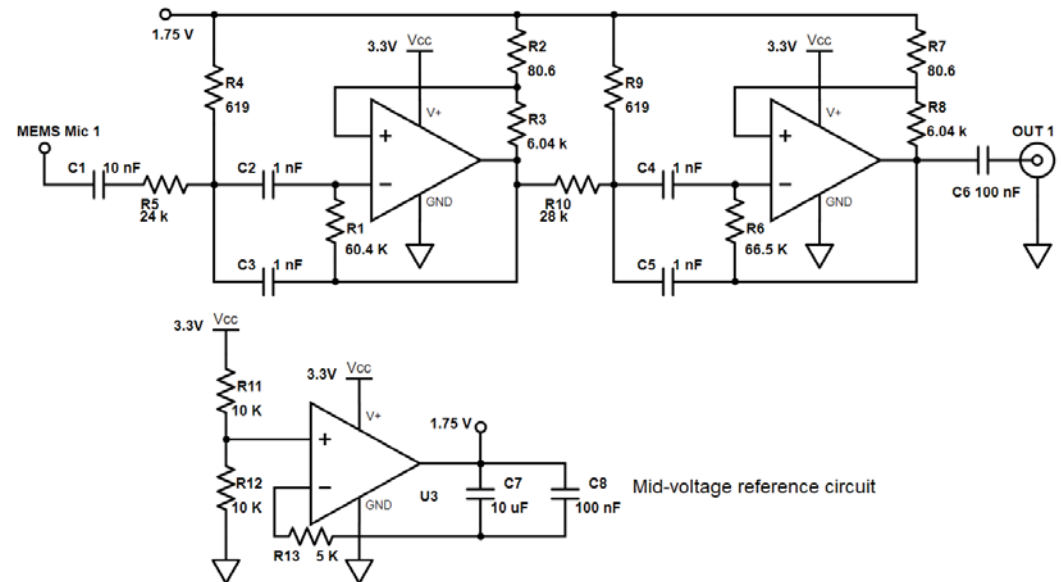
- Low-power and low-cost general purposes capacitive microphone.
- Low dimension $L=3.76$ mm, $W=3.00$ mm, $H=1.10$ mm
- Resonance peak $f_r = 25$ kHz.
- Supply voltage $V = 3.3$ V.



Realization

Reicever filter

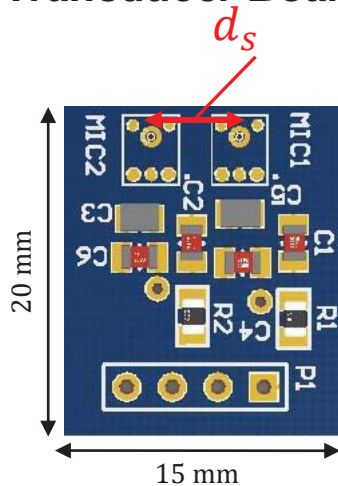
- Single voltage power supply $V_{CC} = 3.3 V$.
- Dual-stage 4th order Chebyshev pass-band filter.
- Central band gain of 14 dB at $f_r = 25 kHz$ and a pass band of 3 kHz.
- Low impedance mid-voltage reference circuit.



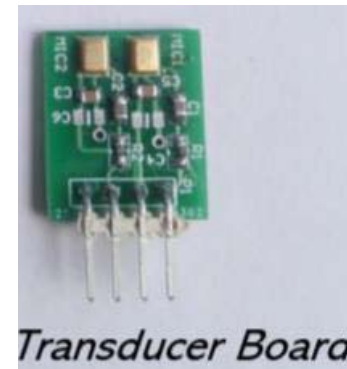
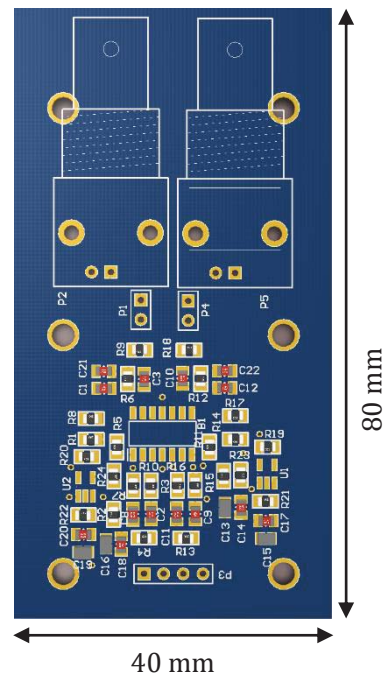
PCB production

Two separate boards were designed. One for the filter and another for the MEMS sensors. The MEMS input aperture distance was: $d_s = (4.9 \pm 0.2) \text{ mm}$.

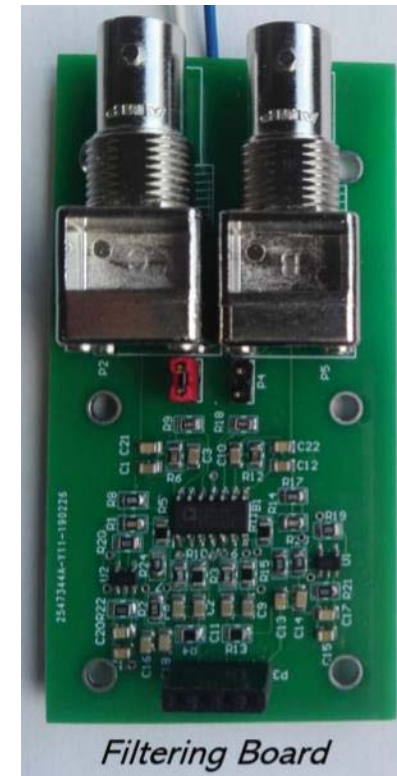
Transducer Board



Filtering Board



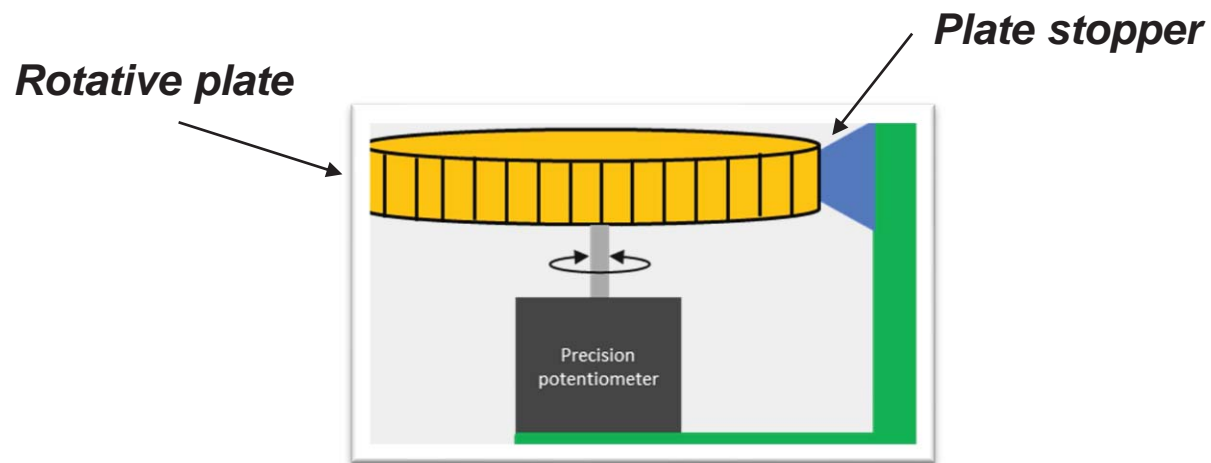
Transducer Board



Filtering Board

Low cost electronics goniometer

A low cost reference heading measurements systems was developed in order to evaluated the heading accuracy of the proposed system.

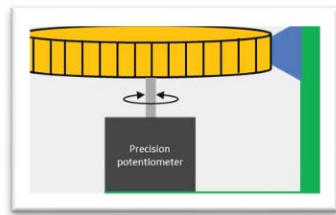


From mechanical consideration the positioning plate angle error is:

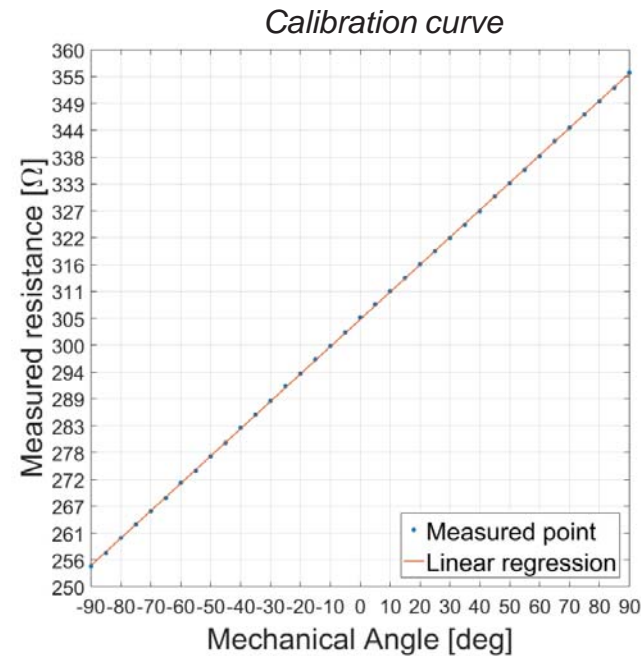
$$\varepsilon = (0.70 \pm 0.06) \text{ deg}$$

Low cost electronics goniometer

Using the mechanical angle position and the measured resistance, an inverse calibration model was applied.



Agilent 34401A



Estimated rotation

Measured resistance

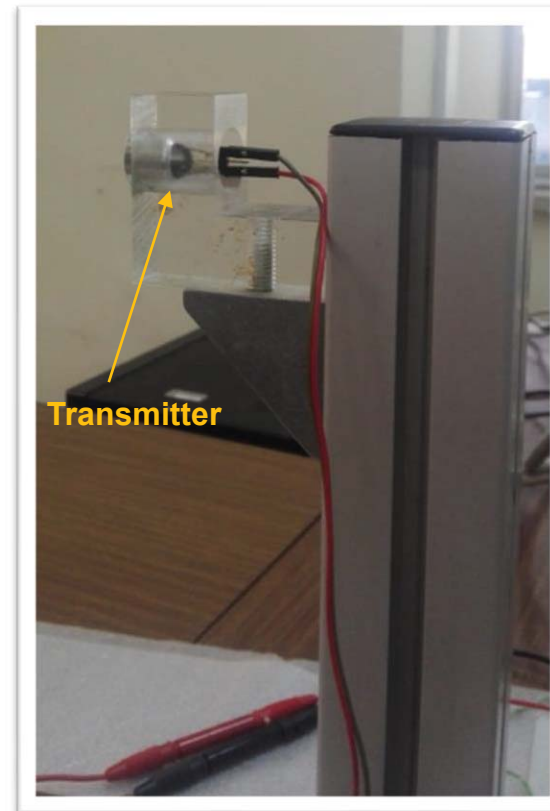
$$\phi = \frac{R - \alpha}{\beta}$$

$$\alpha = 304.57 \Omega$$
$$\beta = 0.56 \Omega/deg.$$

Measurements system

The ultrasonic transmitter was mounted on a plastic holder, supplied by the Arbitrary waveform generator Agilent 33220A.

Continuous $V_{pp} = 3\text{ V}$ sinusoidal signal at the resonance frequency was applied.

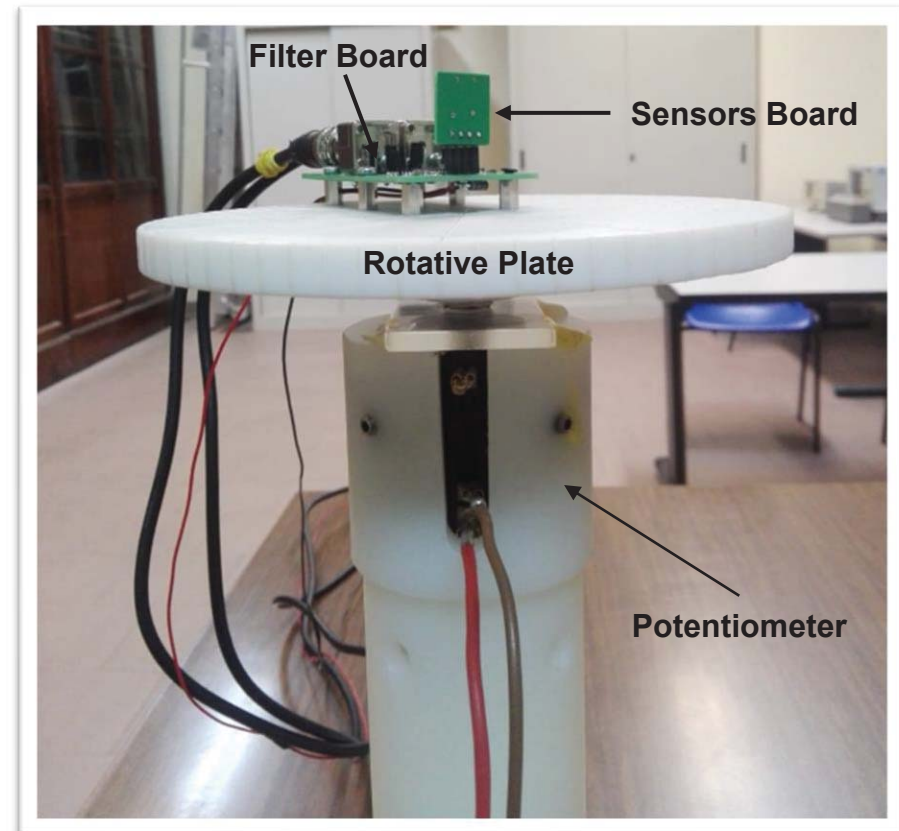


Measurements system

The filter board was mounted on the rotating plate.

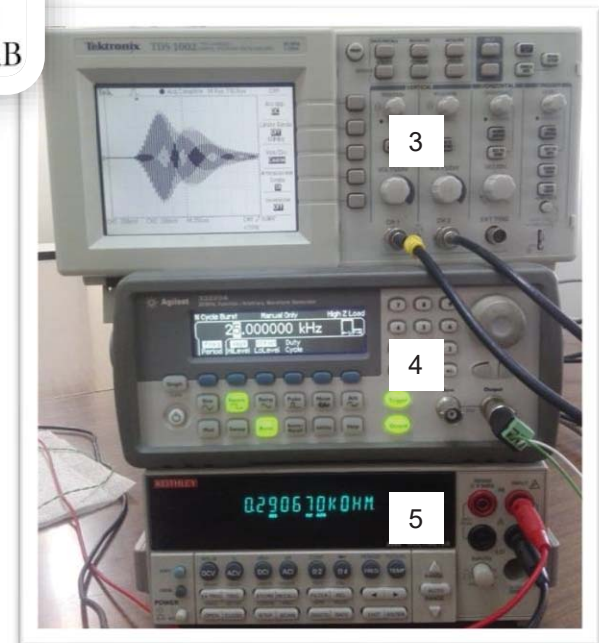
The sensor board centre was aligned at the rotative plate centre.

The signals were acquired by a dual-channel DSO at a sample rate of $f_s = 10$ MHz.



Measurements system

The receivers (1), the transmitter (2), the DSO (3), the waveform generator (4), and the ohmmeter (5).

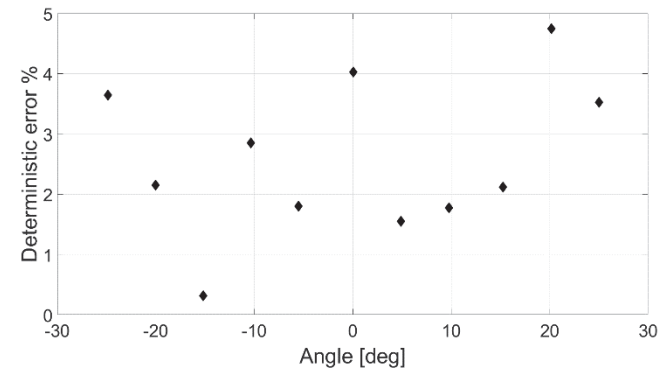
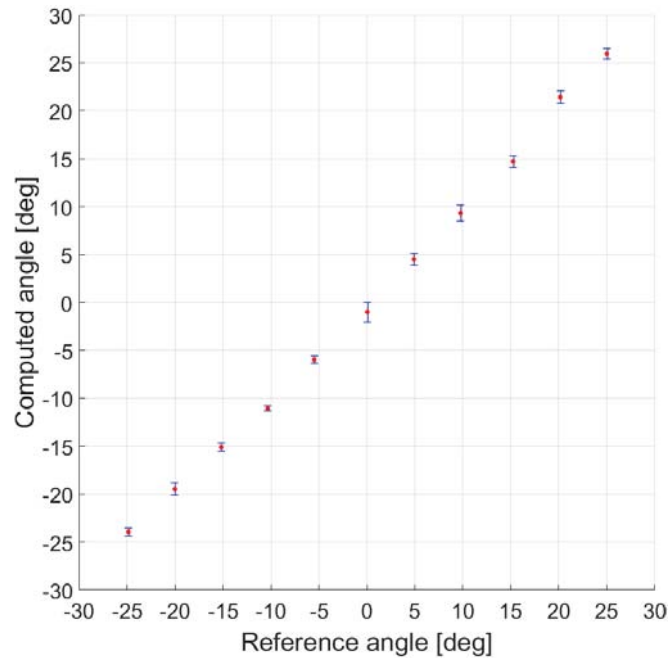


Results



Results

Mean computed angle (.) with standard deviation bar plot [8].



- $\bar{\varepsilon} = 1.2 \text{ deg}$
- $\sigma = 0.8 \text{ deg}$

Comparison

Comparison among the proposed system and recent state-of-the-art solutions based on the same technology, show better performance for the proposed system.

State-of-the-art				
	[9]	[10]	[11]	[12]
Range [deg]	[-40, 40]	[-5, 5]	[-30, 30]	[-20, 20]
Max Error [deg]	<18	<1.5	<2	<3.6
Operation Distance [m]	<4	<1	<1.5	<4

Proposed System	
	Proposal
Range [deg]	[-25, 25]
Max Error [deg]	<1.2
Operation Distance [m]	<7

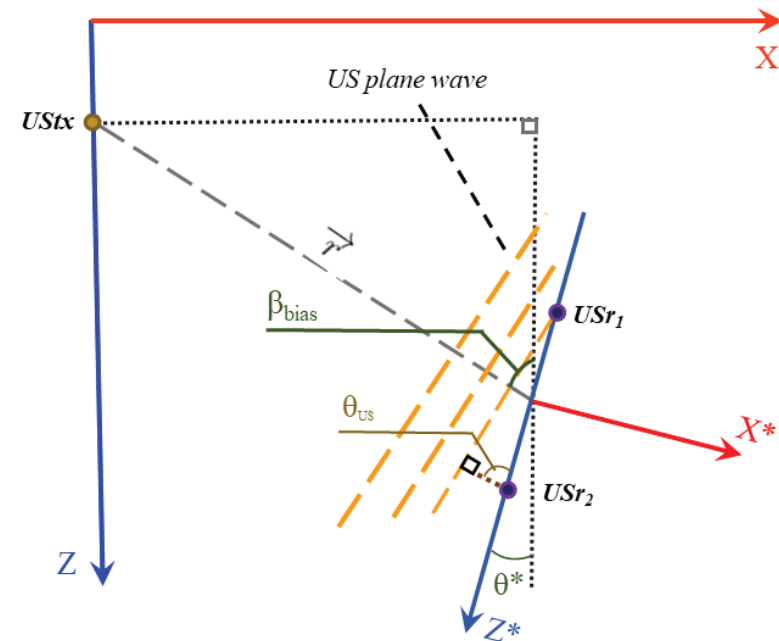
Position effects

The angle estimation uncertainty has two contribute. The positioning contribute was investigated by simulation.

$$\theta^* = \boxed{\beta_{bias}} - \arccos\left(\frac{\delta_{US}}{d_s}\right)$$

$$\beta_{bias} = \arccos\left(\frac{Z_* - Z_{tx}}{|\vec{r}|}\right)$$

Origin localized frame position *US*_{tx} Z position

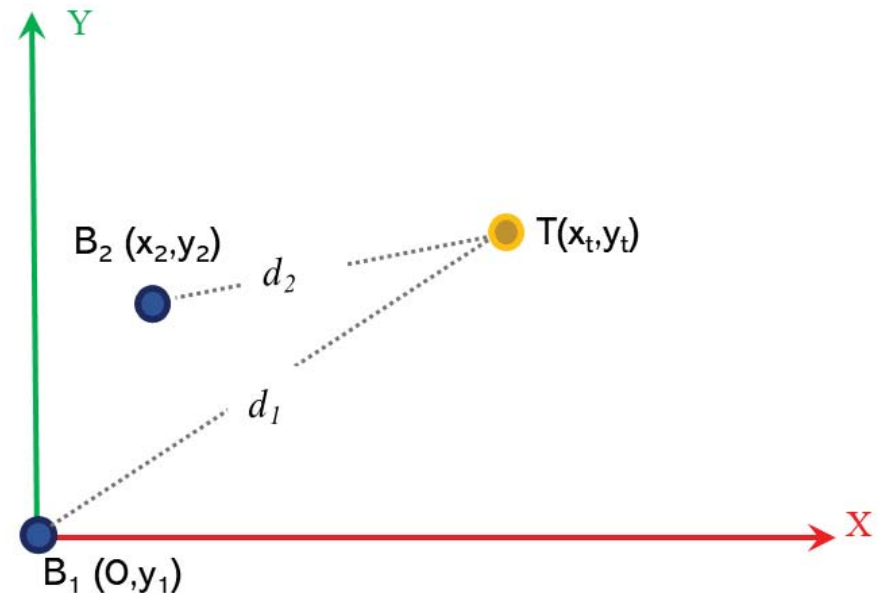


Position effects

The UWB commercial *DecaWaveDW1000* modules were considered (B_{1-2}).

The position was estimated with the trilateration algorithm and the Extended Kalman Filter.

Distance measurements noise standard deviation $\sigma = 10 \text{ cm}$ [13].

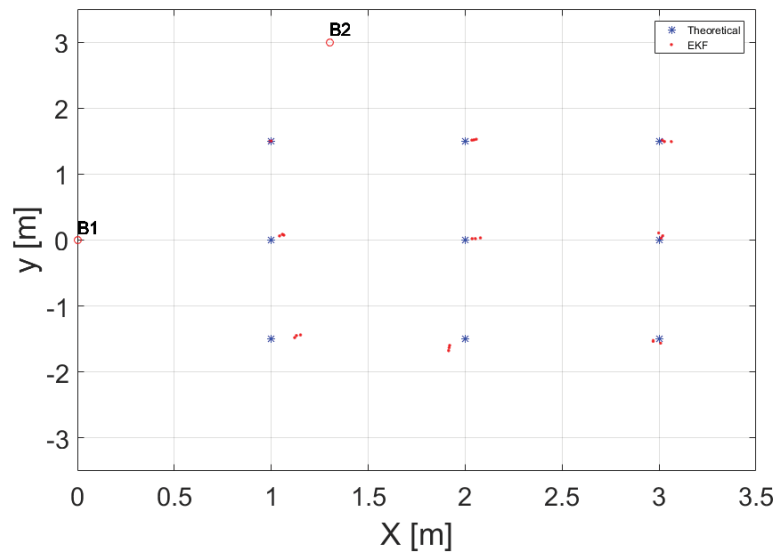


Position effects

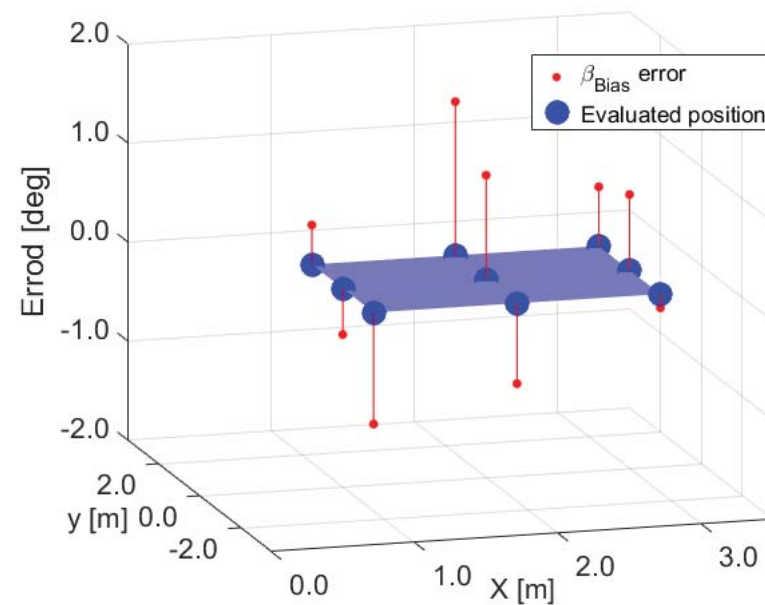
The mean position difference between the reference position (*) and the EKF output (.) was $\varepsilon_{EKF} = 11.5 \text{ cm}$ with a $\sigma_{EKF} = 5.0 \text{ cm}$ standard deviation.

The maximum β_{Bias} mean error was $\varepsilon_{\beta_{Bias}} = 1.1 \text{ deg}$ with a $\sigma_{\beta_{Bias}} = 1.2 \text{ deg}$ standard deviation [14].

Position estimated

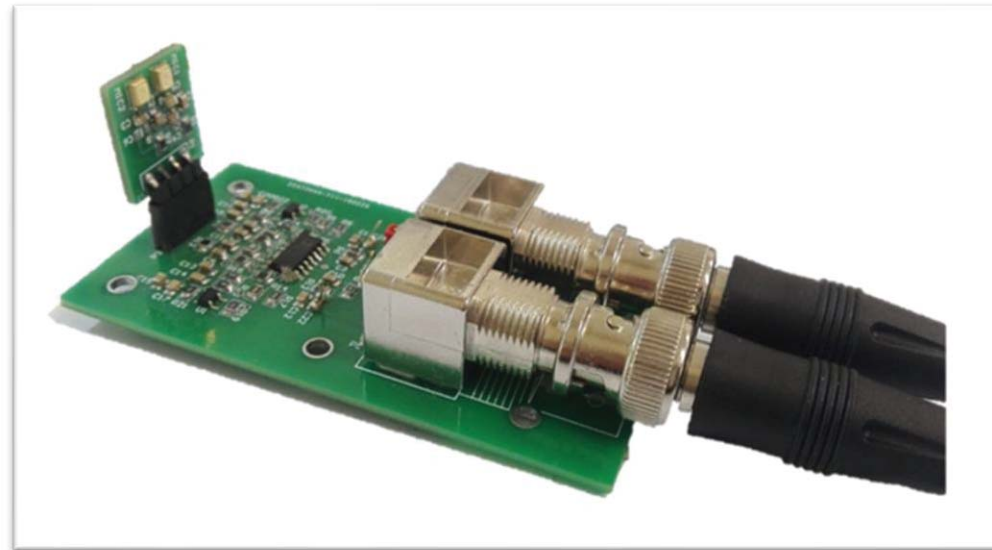


Angles error



Remarks

- ✓ An alternative magnetometer-less heading measurements system is proposed.
- ✓ The metrological performance is comparable with the standard magnetometer solution.
- ✓ The proposed solution needs to know the target position.



Products (I)

- 1) Arpaia, P., Cesaro, U., Gatti, D., & Moccaldi, N. (2020). An ultrasonic heading goniometer intrinsically robust to magnetic interference. **IEEE Transactions on Instrumentation and Measurement**.
- 2) L. Angrisani, P. Arpaia, D. Gatti, A. Masi, and M. Di Castro, "Augmented reality monitoring of robot-assisted intervention in harsh environments at cern," in **Journal of Physics: Conference Series**, vol.1065, no. 17. IOP Publishing, 2018, p. 172008.
- 3) L. Angrisani, P. Arpaia, and D. Gatti. "Analysis of localization technologies for indoor environment." **IEEE International Workshop on Measurement and Networking (M&N)**, 2017.
- 4) L. Angrisani, P. Arpaia, and D.Gatti. "Fast beacon recognition for accurate ultrasonic indoor positioning." **IEEE International Workshop on Measurement and Networking (M&N)**, 2017.

Products (II)

Poster:

- 1) *“Augmented Reality monitoring of robot-assisted intervention in harsh environments at CERN”*. XXII World Congress of the International Measurement Confederation (IMEKO), 3-6 September 2018 Belfast (UK).
- 2) *“Analysis of localization technologies for indoor environment.”* IEEE International Workshop on Measurements and Networking, 27-29 September 2017, University of Napoli Federico II Naples, Italy.

Presentation made:

- 1) *“Fast beacon recognition for accurate ultrasonic indoor positioning”*. IEEE International Workshop on Measurements and Networking, 27-29 September 2017, University of Napoli Federico II Naples, Italy.



THANK YOU FOR YOUR ATTENTION!

